Available online at www.sciencedirect.com
ScienceDirect
Journal of Power Sources 174 (2007) 818–822
JOURNAL OF POWER SOURCES
www.elsevier.com/locate/jpowsour

Short communication

Behaviour of $LiNi_{0.8}Co_{0.2}O_2$-cathodes at high cycle numbers

K. Nikolowski [a,*], N.N. Bramnik [a], C. Baehtz [b], H. Ehrenberg [a], H. Fuess [a]

[a] *Institute for Materials Science, Darmstadt University of Technology, Petersenstr. 23, D-64287 Darmstadt, Germany*
[b] *HASYLAB/DESY, Notkestr. 85, D-22607 Hamburg, Germany*

Available online 27 June 2007

Abstract

In situ synchrotron diffraction experiments were performed to study the behaviour of the cathode material $LiNi_{0.8}Co_{0.2}O_2$ at high cycle numbers. The battery-cell was cycled 140 times between 4.2 and 2.7 V. The initial cycle and several cycles at proceeded degradation of the cell were investigated. In between the cell was cycled *ex situ*. The evolution of the lattice parameters during cycling was determined for the different stages of degradation by means of Rietveld refinement. Comparing the initial cycle of the cell with the higher cycle numbers, the mechanism of lithium insertion/extraction does not change significantly. But, the range in which the lattice parameters change during one cycle becomes smaller. This can be attributed to interface layer formation and to slightly less lithium exchange in the same voltage window.
© 2007 Elsevier B.V. All rights reserved.

Keywords: Lithium-ion battery; Cathode material; *In situ* diffraction; Degradation; $LiNi_{0.8}Co_{0.2}O_2$; Layered structure

1. Introduction

X-ray diffraction is a powerful method for materials characterisation. It can provide useful chemical information like phase composition, information on the particle morphology like crystallinity, particle shape and particle size and structural information like lattice parameters, atomic positions, thermal displacement parameters, etc.

Our intention in the field of *in situ* diffraction was to get high quality diffraction data to be able to extract as much information as possible on the above mentioned parameters *during* cycling. In a previous paper [1], we extracted lithium nearly completely from the cathode material $LiNi_{0.8}Co_{0.2}O_2$ and presented microstructural investigations performed with *in situ*-diffraction. Regarding the study of the degradation of a cathode material, most experiments described in literature are performed *post mortem*. This leads to information concerning the properties of the cycled material. For this contribution, we have used *in situ*-diffraction to detect also possible changes in the mechanism of lithium insertion/extraction due to the degradation of the cathode material.

$LiNi_{0.8}Co_{0.2}O_2$ is well known as a positive electrode material for lithium batteries [2–9]. It crystallizes in the space group R-3m. Assuming a perfectly ordered structure, alternating Li- and Ni/Co-layers are separated by oxygen-layers. The material has a theoretical capacity of 274 mAh/g. One crucial factor influencing the electrochemical behaviour of this material - and layered materials with the sum-formula $LiMO_2$ (M = Ni, Co, Mn) in general—is the amount of 3d-ions on the lithium slab, referred to as cation disorder. The cation disorder is mainly influenced by the synthesis temperature and by the nature of the ions present on the 3d-metal-layer [9].

For this contribution we used our optimized synchrotron diffraction *in situ*-cell described in [10] to investigate the behaviour of the cathode material $LiNi_{0.8}Co_{0.2}O_2$ at high cycle numbers. During cycles 1, 53–56 and 138–140 about 25 diffraction patterns were collected per cycle. The lattice parameters were refined by the Rietveld-method and their evolution is discussed in dependence on the charge/discharge state and the cycle number, respectively.

2. Experimental

$LiNi_{0.8}Co_{0.2}O_2$ was prepared by a modified Pechini-synthesis as described in detail elsewhere [1,9]. The final annealing temperature was 775 °C for 10 h. In order to characterize the obtained powder, X-ray diffraction patterns where collected on a laboratory diffractometer (STOE StadiP) operating in transmission mode. The powder was found to be single phase $LiNi_{0.8}Co_{0.2}O_2$, crystallizing in the spacegroup R-

* Corresponding author.
E-mail address: nikolowski@st.tu-darmstadt.de (K. Nikolowski).

0378-7753/$ – see front matter © 2007 Elsevier B.V. All rights reserved.
doi:10.1016/j.jpowsour.2007.06.090

3m. The lattice parameters and the oxygen z-coordinate were refined with the Rietveld-method using the WinPlotR software package [11]. The refinement of the lattice parameters lead to the following values: $a = 2.86655(6)$Å, $c = 14.1715(5)$Å and $z_{oxygen} = 0.25826(29)$. In order to take in account the cation disorder, nickel was allowed to move from the 3b to the 3a-site, but the total amount of nickel was constrained. The percentage of nickel ions situated on the lithium site was determined to be approximately 2.8% for the pristine material.

For the *in situ*-diffraction studies, the cathode material $LiNi_{0.8}Co_{0.2}O_2$ was ground together with carbon black and PVDF and pressed into a pellet of 19.2 mg. The experiments were carried out using a dedicated *in situ*-cell for battery cycling described in [10] at beamline B2 [12] of the Hamburger Synchrotronstrahlungslabor (HASYLAB@DESY, Germany, http://www-hasylab.desy.de). Metallic lithium was used as anode, aluminum as current collector on the cathode side and a 1M solution of $LiPF_6$ in EC:DMC = 2:1 (Ferro Corp.) as electrolyte. A wavelength of $\lambda = 0.5006$ Å was selected by a doublecrystal Si(1 1 1) monochromator. For the data acquisition the on-site readable imageplate detector OBI was used [13]. Full pattern Rietveld refinement of the structural parameters for all *in situ*-diffraction patterns was performed using the WinPlotR software package [11]. The *in situ*-cell was cycled in constant-current mode between 4.2 and 2.7 V, controlled by a VMP multichannel potentiostat (Bio-Logic, Princeton Applied Research).

3. Results and discussion

The charge and discharge capacities of the *in situ*-cell during cycling are shown in Fig. 1. There are three sections in which *in situ* X-ray diffraction experiments were performed: cycle 1, cycles 53–56 and cycles 138–140. Upon these experiments the discharge capacities dropped from 161 mAh/g (cycle 1) to 142 mAh/g (cycle 54) and finally to 124 mAh/g (cycle 139). This corresponds to capacity retention of approximately 77% after 140 cycles. For all *in situ* cycles the same current rate of C/5 was used.

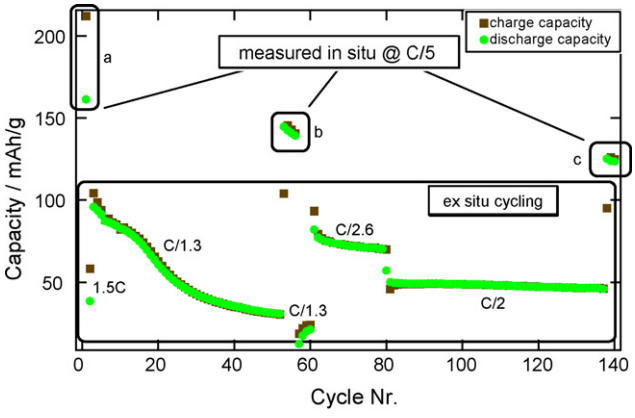

Fig. 1. Charge and discharge capacities during cycling of the *in situ*-cell. The cycles measured by *in situ*-XRD are labeled with a, b and c. The measured X-ray diffraction patterns are shown in Fig. 2.

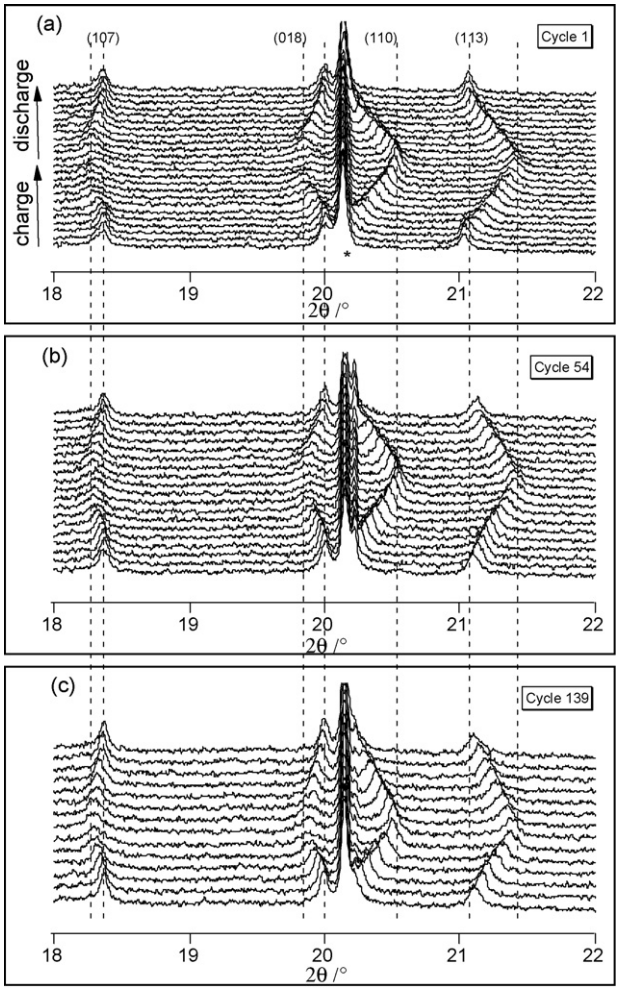

Fig. 2. X-ray diffraction patterns measured *in situ* during cycling of $LiNi_{0.8}Co_{0.2}O_2$. The cycles marked with a, b and c in Fig. 1 (cycles 1, 54 and 139, respectively) are shown. The chosen wavelength was $\lambda = 0.500640$ Å. The 107, 018, 110 and 113 reflections are indicated; the reflection marked with (*) is from aluminium used as current collector on the cathode side. The evolution of the 113-reflection during the first charging reflects the initial two-phase behaviour.

Between the *in situ*-diffraction experiments, the cell was cycled *ex situ*. During these periods, the current rate was increased in order to reach a higher cycle number in a reasonable time. Upon cycling, the rate capability of the cell decreased. To keep the amount of lithium extracted/inserted approximately constant, the current rate was adjusted as it is noted in Fig. 1.

As representatives the diffraction patterns collected during cycles 1, 54 and 139 are shown in Fig. 2 as waterfall-plots. In each plot, from bottom to top the cell is first charged and then discharged. For sake of clarity only a small section of the diffraction patterns is shown (18–22° in 2θ) while the whole pattern was collected (5–45° in 2θ) and considered in the Rietveld refinement. In this 2θ-window the indexed reflections are: 107, 018, 110 and 113. In addition, one aluminium reflection marked with an asterisk is visible in the figure. During the charge process, the two reflections with a high l-value, e.g. the 107 and 018 reflections, move to lower 2θ-values, reflecting the expansion of the c-axis. Whereas the two reflection with a low l-value,

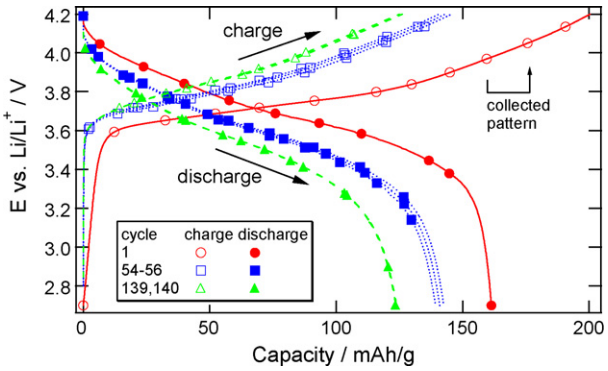

Fig. 3. Charge and discharge curves of the *in situ*-cell. The points indicate the periods during which one diffraction pattern was measured. The points indicate the end of the measuring time.

e.g. the 110 and 113 reflection, move two a higher value of 2θ, which indicates a contraction of the *a*- and *b*-axis. During discharge the reflections move back to their initial 2θ-positions. This behaviour is consistent with previous reports [4,9,14–17]. The changes of the lattice parameters during the cycles will be discussed in detail later in this paper using the parameters determined by Rietveld-refinement.

The dashed lines in Fig. 2 show the range in which the reflection positions change during the charge/discharge process. Comparing the three cycles, this range becomes slightly narrower going from cycle 1 to cycle 54 and cycle 139.

The charge and discharge profiles of the cell during the *in situ*-measurements are shown in Fig. 3. In Fig. 3 and for the further structural investigations, only cycles 1, 54–56 and 139–140 where evaluated. The symbols on the charge and discharge curves indicate the exposure periods for each diffraction pattern.

In Fig. 4 the differential capacities for the cycles 1, 54 and 139 are shown. Since the cycling experiments were performed galvanostatically, electrochemical data points were collected either after the voltage changed by a given interval ($dE = 5$ mV) or after a certain time ($dt = 300$ s). The second condition was applied in order to collect data even when the voltage does not change, e.g. on a voltage-plateau. Due to these experimental conditions dQ, which is plotted in Fig. 4 as a function of the cell voltage E, shows the charge flown between two recorded data points

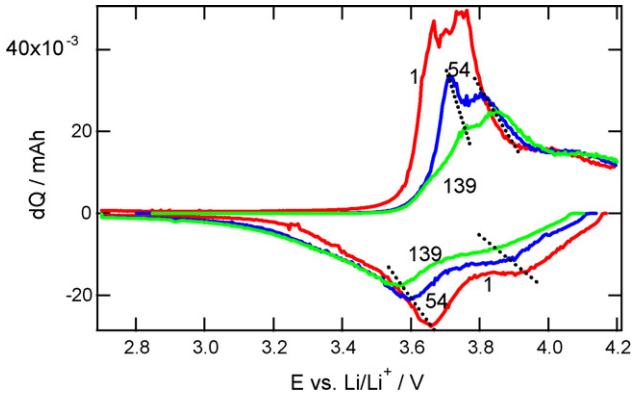

Fig. 4. Derivatives of the cycles 1, 54 and 139 shown in Fig. 3. The decrease and shift of the oxidative and reductive peaks is indicated by the dotted lines.

and cannot be unambiguously associated to a given voltage step. Nevertheless, the plot is used to emphasize the changes in the charge–discharge-curves shown in Fig. 3. Three oxiditative peaks appear in Fig. 4 at approximately 3.6 and 3.8 V and a broad one at approximately 4.1 V. With increasing cycle number the area under the peaks (especially under the first one) decreases and the peaks shift to higher voltages. At the same time the peak intensities of the reductive peaks decrease and shift to lower voltages. This behaviour indicates the increasing polarisation (caused by an increase of the cell-resistance) at higher cycle numbers. In comparison, the analogous peaks in two CV-experiments [4,18] show a decrease in peak-area but a significantly lower shifting. So, the increase in polarisation seems to be associated to the specific setup or the specific conditions of cycling.

The lattice parameters a and c, refined by full-pattern Rietveld-analysis of the diffraction patterns measured during cycling of the cell, as well as the unit-cell volume V are shown in

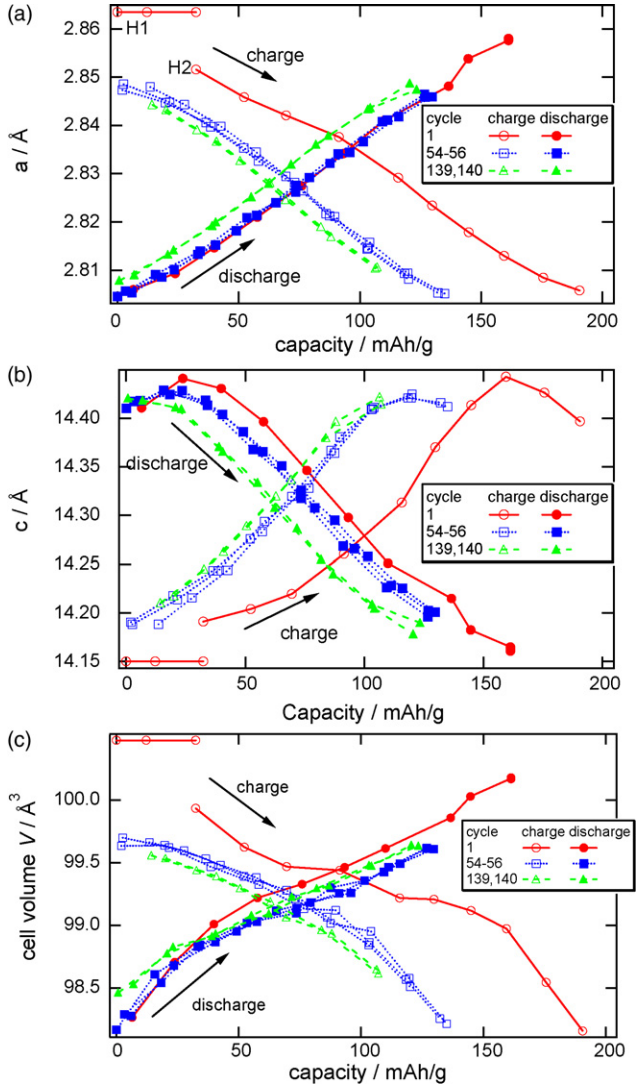

Fig. 5. Development of (a) lattice constant a (the to phases H1 and H2 are indexed); (b) lattice constant c; and (c) unit cell volume V as a function of the charge- or discharge capacities, respectively.

Fig. 5a–c. They are plotted for the cycles 1, 54–56 and 139–140 as functions of the charge and discharge capacities, respectively. Note, that the cell was cycled in constant-current mode without relaxation periods at the end of the cycles, so that the lattice parameters could not be determined in all cases exactly at the beginning and at the end of a charge or discharge process, respectively (see Fig. 4 for the periods, in which the diffraction patterns were collected).

At the beginning of the first charge, the pristine Phase H1 converts into a second phase H2. Both phases are isostructural but differ in their lattice parameters. This two phase-behaviour was described in detail earlier for $Li_xNi_{0.8}Co_{0.2}O_2$ [1,9,15–17], as well as for Li_xCoO_2 [19,20] and $LiNiO_2$ [21], and is illustrated in the evolution of the 113-reflection during the first charge in Fig. 2. The lattice parameters of H1 were refined for the first measured diffraction pattern and then constrained for the second and third pattern. Phase H2 was included in the refinement in pattern three and was the dominant phase in pattern four. At this point (x_{Li} is approximately 0.8) the phase-ratio of H1:H2 is smaller than 0.2:0.8. Beginning with the fourth pattern the extraction/insertion of lithium proceeds via a solid-solution mechanism.

Generally, the evolution of the lattice parameters for the first charge shows a significant difference compared to the later ones. During the charge of cycle 1 parts of the charge capacity seem to be consumed by formation or conditioning processes, resulting in a capacity loss, which shifts the curve to higher capacity values. During cycles 54–56 these processes are already completed and the positions of the curves for the charging in cycles 54–56 and 139–140, respectively, are similar.

When lithium is extracted during the charge process, the lattice parameter *c* expands due to the increasing coulomb repulsion between the oxygen layers up to a lithium concentration of approximately $x_{Li} = 0.4$ in $Li_xNi_{0.8}Co_{0.2}O_2$ and then contracts on further lithium extraction. This behaviour is most pronounced in the first cycle, where the *c*-axis clearly shows a maximum at a charge capacity of approximately 160 mAh/g (Fig. 5b). For the cycles 54–56, this maximum is shifted to smaller discharge capacities: of approximately 120 mAh/g. For the last measured cycles 139 and 140 the *c*-axis does not contract during charging at all. The lattice parameter *c* reaches its maximum at about 110 mAh/g. The maximal expansion during the first charge is in good agreement with the results from Ronci et al. [16], who reported, that the maximum in their experiment is at $x_{Li} = 0.35$. Since they charged the cell up to 4.5 V for cycles 1–3 and then steadily increased the upper cut-off voltage to 4.9 V during cycles 4–7, these measurements are not directly comparable. On the beginning of the discharge this behaviour is reversed. While the lattice parameter *c* for cycle 1 first expands, reaches a maximum and then contracts, this maximum is less pronounced for the cycles 54–56 and not present at all for the cycles 139 and 140. If this maximum is directly linked to the extraction of lithium up to a specific lithium-content (e.g. up to approximately $x_{Li} = 0.4$ in $Li_xNi_{0.8}Co_{0.2}O_2$), the amount of lithium remaining in the structure increases with increasing cycle number. This behaviour may be due the mentioned increase of the cell-resistance due to modifications on the interfaces leading to an effective voltage loss. So, at the final voltage of 4.2 V different amounts of lithium would remain in the host material.

As to the final values of the unit cell volume *V* reached during charging, nearly the same cell volume is reached in the first cycle and in cycles 54–56 ($V_{cycle\ 1}$ and $V_{cycles\ 54–56} = 98.2\ Å^3$) but in cycles 139-140 the cell volume contracts only to $V_{cycles\ 139–140} = 98.5\ Å^3$. This is in agreement with the contraction of the *c*-axis after the initial expansion which is not observed for cycles 139–140, and the explanation, that the amount of residual lithium increases as discussed above. During discharge, the cell volumes in cycles 139–140 are larger compared to cycles 1 and 54–56, as consequence of the former charge process, but all cycles show a similar progression with respect to the discharge capacity.

In our previous study [1] we reported the complete extraction of lithium up to x_{Li} is close to 0 in $Li_xNi_{0.8}Co_{0.2}O_2$. After the reinsertion the lattice parameter *a* and *c* and the cell volume almost returned to their initial values. In this experiment the cell volume before (100.48 $Å^3$) and after one cycle (100.18 $Å^3$) are quite close, although not as close as in the former experiment. This may be due to the higher C-rate (C/15 for the experiment in [1] and C/5 for this experiment, respectively). In comparison Ronci et al. [16] report a significant difference between the lattice parameters *a* and *c* determined at the beginning and the end of the first and the second cycle, although they used an even lower C-rate of C/72. But, as mentioned above, the cell was charged up to a higher potential, and no information was given about the evolution of the values at the beginning and the end of cycles measured after prolonged cycling.

4. Conclusions

The minimum concentration x_{Li} in $Li_xNi_{0.8}Co_{0.2}O_2$ during charge seems to be similar for cycles 1 and cycles 54–56, keeping in mind, that during cycle 1 formation processes occur. After further cycling, the minimum amount of lithium seems to be larger. This is deduced from the values at the end of the charging of the lattice parameters and the unit cell volume which are different for cycles 139–140 compared to cycle 1 and cycles 54–56. The effect could be due to the higher polarization because of the formation of surface films on prolonged cycling, but also structural changes (microstructure, cation distribution) can be assumed. On the discharge, the reasons for the decreasing delivered capacities seem to be firstly, that lithium cannot be inserted into the host material to the same extent in the later cycles compared to cycle 1. This is for example reflected by the value of *V* after the discharge for cycle 1 which is not reached in the later cycles. Secondly, that in the last measured cycles 139–140 less lithium was extracted, as compared to cycles 1 and 54–56, and so less lithium could be reinserted, leading to the reduced delivered capacities.

In situ X-ray diffraction was successfully used to study the behaviour of the cathode material $Li_xNi_{0.8}Co_{0.2}O_2$ at different cycle numbers. In addition to the conclusion, that the structure of the material is maintained, it can be deduced from the *in situ* experiments that the mechanism of lithium extraction/insertion

from/into the host material does not change significantly upon the examined cycles, e.g. up to cycle number 140.

Acknowledgements

This work was financially supported by the Deutsche Forschungsgemeinschaft in the frame of project SFB 595 'Electrical Fatigue in Functional Materials'. The development of dedicated *in situ* setups for materials characterization using synchrotron radiation is the task of the 'Virtual Institute' VH-VI 102 within the Helmholtz Society of Research Centres.

References

[1] K. Nikolowski, N.N. Bramnik, C. Baehtz, H. Ehrenberg, H. Fuess, ECS Trans. 1 (2006) 17–26.
[2] I. Saadoune, C. Delmas, J. Mater. Chem. 6 (1996) 193–199.
[3] I. Saadoune, C. Delmas, J. Solid State Chem. 136 (1998) 8–15.
[4] E. Levi, M.D. Levi, G. Salitara, D. Aurbach, R. Oesten, U. Heider, L. Heider, Solid State Ionics 126 (1999) 97–108.
[5] R.K.B. Gover, R. Kanno, B.J. Mitchell, M. Yonemura, Y. Kawamoto, J. Electrochem. Soc. 147 (2000) 4045–4051.
[6] R.K.B. Gover, R. Kanno, B.J. Mitchell, A. Hirano, Y. Kawamoto, J. Power Sources 97 (8) (2001) 316–320.
[7] H. Liu, J. Li, Z. Zhang, J. Solid State Electrochem. 7 (2003) 456–462.
[8] H. Liu, Z. Zhang, Z. Gong, Y. Yang, Solid State Ionics 166 (2004) 317–325.
[9] T. Gross, T. Buhrmester, K.G. Bramnik, N.N. Bramnik, K. Nikolowski, C. Baehtz, H. Ehrenberg, H. Fuess, Solid State Ionics 176 (2005) 1193–1199.
[10] K. Nikolowski, C. Baehtz, N.N. Bramnik, H. Ehrenberg, J. Appl. Cryst. 38 (2005) 851–853.
[11] T. Roisnel, J. Rodríguez-Carvajal, Mater. Sci. Forum 378–381 (2001) 118–123.
[12] M. Knapp, C. Baehtz, H. Ehrenberg, H. Fuess, J. Sync. Rad. 11 (2004) 328–334.
[13] M. Knapp, V. Joco, C. Baehtz, H.H. Brecht, A. Berghaeuser, H. Ehrenberg, H. von Seggern, H. Fuess, Nucl. Instrum. Methods A521 (2004) 565–570.
[14] M. Balasubramanian, X. Sun, X.Q. Yang, J. McBreen, J. Power Sources 92 (2001) 1–8.
[15] V.R. Albertini, P. Perfetti, F. Ronci, P. Reale, B. Scrosati, Appl. Phys. Lett. 79 (2001) 27–29.
[16] F. Ronci, B. Scrosati, V.R. Albertini, P. Perfetti, J. Phys. Chem. B 105 (2001) 754–759.
[17] V.R. Albertini, P. Perfetti, F. Ronci, B. Scrosati, Chem. Mater. 13 (2001) 450–455.
[18] K.S. Tan, M.V. Reddy, G.V. Subba Rao, B.V.R. Chowdari, J. Power Sources 141 (2005) 129–142.
[19] J.N. Reimers, J.R. Dahn, J. Electrochem. Soc. 139 (1992) 2091–2097.
[20] M. Morcrette, Y. Chabre, G. Vaughan, G. Amatucci, J.-B. Leriche, S. Patoux, C. Masquelier, J.-M. Tarascon, Electrochim. Acta 47 (2002) 3137–3149.
[21] X.Q. Yang, X. Sun, J. McBreen, Electrochem. Comm. 1 (1999) 227–232.